2005 WJTA American Waterjet Conference
August 21-23, 2005 • Houston, Texas

Paper 3A-2

DETERMINATION OF ABRASIVE PARTICLE VELOCITY USING LASER-INDUCED FLUORESCENCE AND PARTICLE TRACKING METHODS IN ABRASIVE WATER JETS

P. Roth, H. Looser, K.C. Heiniger, S. Bühler
University of Applied Sciences Aargau FHA
CH-5210 Windisch, Switzerland

ABSTRACT

In AWJ cutting heads an abrasive water jet is formed by mixing abrasive particles with a high-speed water jet. In order to understand the physics of this mixing process, knowledge of the velocity of the abrasive particles at the exit of the focusing tube is of major importance. In literature, different models describing the cutting process or parts of it can be found where the velocity of the abrasive particles is a key parameter.
Up to now, various methods have been applied to experimentally investigate the particle velocity or the acceleration process in the focusing tube. However, none of these experiments were carried out under real conditions typical for today's AWJ cutting.
In this paper we present a new technique with which we are able to determine the velocity of abrasive particles under real AWJ cutting conditions. The technique is a modification of the well known particle tracking velocimetry. It is based on two key issues: Use of abrasive particles coated with a thin layer of fluorescent dye and the application of a sophisticated, nonlinear image processing algorithm. Standard image processing algorithms fail because some of the dye detaches from the abrasive particles and this results in an extensive background noise which makes it prohibitive to detect the particle by linear algorithms.

1. INTRODUCTION

The abrasive waterjet (AWJ) cutting technique is based on accelerating small diameter abrasive particles through a high velocity water jet to remove material.

Water is pumped to high pressures (>250MPa) and a water jet is formed by a sapphire or diamond orifice of diameter 0.1÷0.4mm. Downstream from the orifice, abrasive particles are added in a mixing chamber and accelerated by momentum exchange with the water jet in a focusing tube. From there they are directed to the workpiece (**Figure 1**).

Several studies investigated the AWJ material removal process, which essentially is an erosion process. Hashish [1] has developed a model based on the physical parameters involved for predicting the cutting depth in brittle materials:

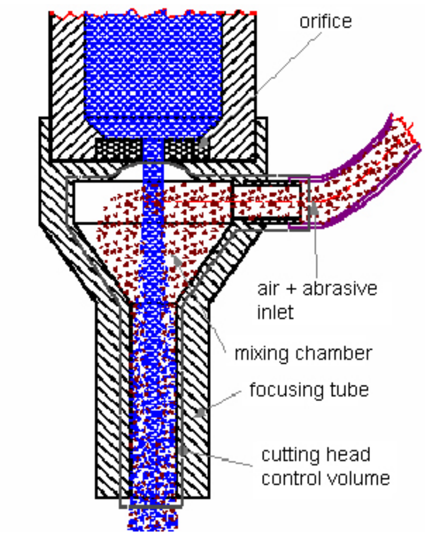

Figure 1 AWJ cutting head

$$h = \frac{2 \cdot \left((1-c) \cdot \dot{m} \cdot v^2 \right)}{\pi \cdot d_j \cdot \varepsilon \cdot \mu} \qquad (1)$$

with following parameters:

h	cutting depth	[m]
μ	traverse rate of the jet	[m/s]
c	material dependant constant	[-]
$\dot{m}$	abrasive mass flow	[kg/s]
v	abrasive particle velocity	[m/s]
d_j	water jet diameter	[m]
ε	specific energy of material	[J/m^3]

Bitter [2] published an equation for the volume of removed material in erosion for brittle materials:

$$V = \frac{1}{2} \cdot \frac{m \cdot \left((v \cdot \sin(\alpha)) - K \right)^2}{\varepsilon} \qquad (2)$$

with following variables:

V	removed volume	[m^3]
m	total mass of particle impacted	[kg]
v	particle velocity	[m/s]
α	angle of particle impact	[deg]
K	constant dependant on the material eroded and the properties of the abrasive particles	[-]
ε	specific energy of material	[J/m^3]

From these correlations it follows that the velocity of the abrasive particles is of prime importance for the cutting performance. Additionally, the abrasive mass flow rate is a relevant parameter, affecting the particle velocity, and thus the cutting performance.

1.1 Objectives

The main objective of this paper is to describe a new method for measuring the velocity of abrasive particles in AWJ under real conditions. Instead of using steel shot and a coil, as done in previous studies [3, 4, 5], abrasive particles coated with a fluorescent dye have been used. The fluorescent layers are excited by a pulsed laser and the emitted radiation is detected by a CCD camera. Finally the velocity is computed by a particle tracking velocimetry (PTV) algorithm.

With this new method experiments were performed with varying water pressure and abrasive mass flow rate, while keeping the cutting geometries constant. The effects of these two parameters on the particle velocity and the AWJ process are discussed in section 3.

2. EXPERIMENT

2.1 Particle tracking with laser-induced fluorescence (LIF)

The principle of laser-induced fluorescence is to excite the electrons of the atoms or molecules of a dye with photons from a laser. The excited electrons then generally return to the ground state by a multistep process (**Figure 9**). In consequence, the wavelength of the re-emitted radiation is larger than the excitation wavelength. When imaging objects coated with a fluorescent dye, the excitation radiation from the laser is efficiently suppressed by the use of a long pass filter and thus all nonfluorescent objects are suppressed in the image taken by the camera.

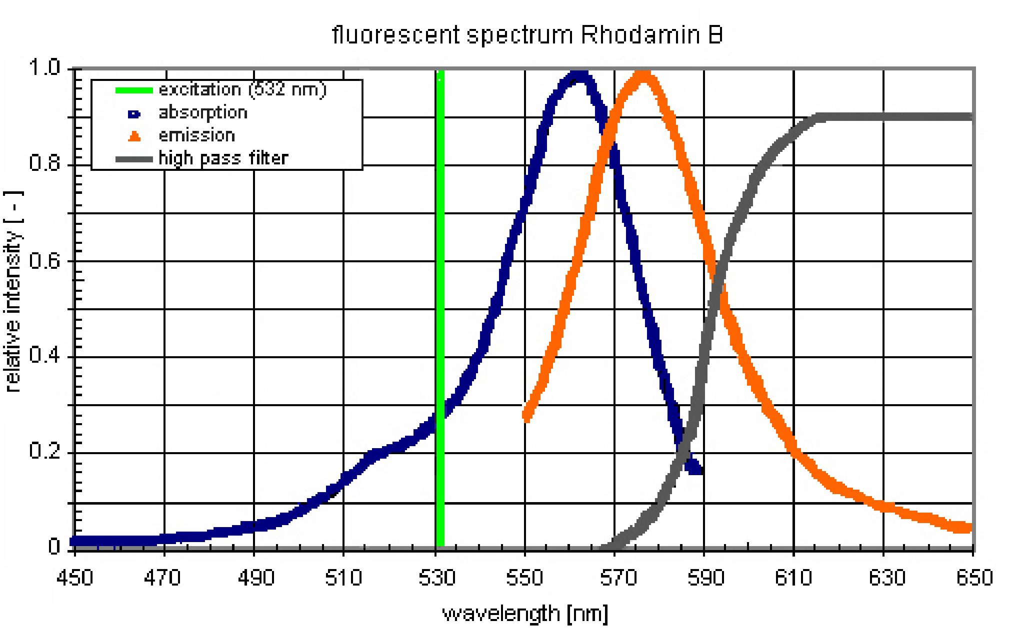

Figure 2 Fluorescence spectrum

For this application, a synthetic dye called Rhodamin B ($C_{28}H_{31}ClN_2O_3$) was used. **Figure 2** shows both the absorption and emission spectrum of the dye together with the excitation wavelength (532 nm) and the transmission curve of the long pass filter used in these experiments.

2.2 Velocity evaluation using particle tracking velocimetry (PTV)

The abrasive waterjet with coated particles was illuminated by a double pulse from a frequency doubled Nd:YAG laser. The time delay between the two laser pulses of 120 mJ/5 ns at 532 nm was set to 1 microsecond. With a fast frame-transfer CCD camera, equipped with a long pass filter, two images of the fluorescent waterjet with abrasive particles were taken. Image processing these "double images" (see chapter 2.3) then revealed the displacement of the particles within the time delay of the laser pulses and thus allowed us to compute the velocity of the particles.

2.3 Image processing

The identification of the fluorescent particles in the abrasive waterjet by image processing proofed to be a formidable task, because some of the dye detached from the abrasive particles and created a large background noise as can be seen from **Figures 3/4**. Linear methods like averaging or 2D-bandpass filtering and subsequent thresholding showed to be ineffective: Either most of the particles remained undetected or a large number of "ghost particles" were created. In addition, inspection of the unprocessed images by eye was not feasible due to the large number of images without any particle.

The finally successful image processing program is composed of six major steps:

Step 1	Median Filter
Step 2	Rolling Rugby Ball Filter
Step 3	Bandpass Filter
Step 4	Rolling Rugby Ball Filter
Step 5	Standard particle detection with a threshold of 5 times the standard deviation of the pixel intensity and a minimum particle size of 150 pixels (in the 250 x 512 pixel images)
Step 6	Check for particle pairs with a maximum sidewise displacement of 20 pixels.

The key feature of the program is the *nonlinear background subtraction algorithm* that we named "rolling rugby ball filter" and that was developed for this work. It is a modification of the rolling ball filter implemented for example in the open source program "ImageJ" [6, 7].
For the purpose of explaining the algorithm, imagine that the 2D grayscale image has a third dimension (height) defined by the intensity value at every point in the image. The center of the filtering object, a patch from the top of a sphere with suitable diameter *d*, is moved along each scan line of the image so that the patch is tangent to the image at one or more points, with every other point on the patch below the corresponding point of the image. The moving center of the sphere thus describes a surface which is considered to be the background (plus a constant).

Figure 3 demonstrates this process on an intensity profile across the waterjet. From this figure it becomes clear that structures, with characteristic lengths larger than the diameter of the sphere, will be removed efficiently while small structures are preserved. In our images however, the background consisted of "hill trains", elongated in the direction of the waterjet. Unfortunately, the average width of these hill trains was equal to the average particle diameter. In consequence, removing the hills by choosing a suitable diameter for the rolling sphere also removed the particles.

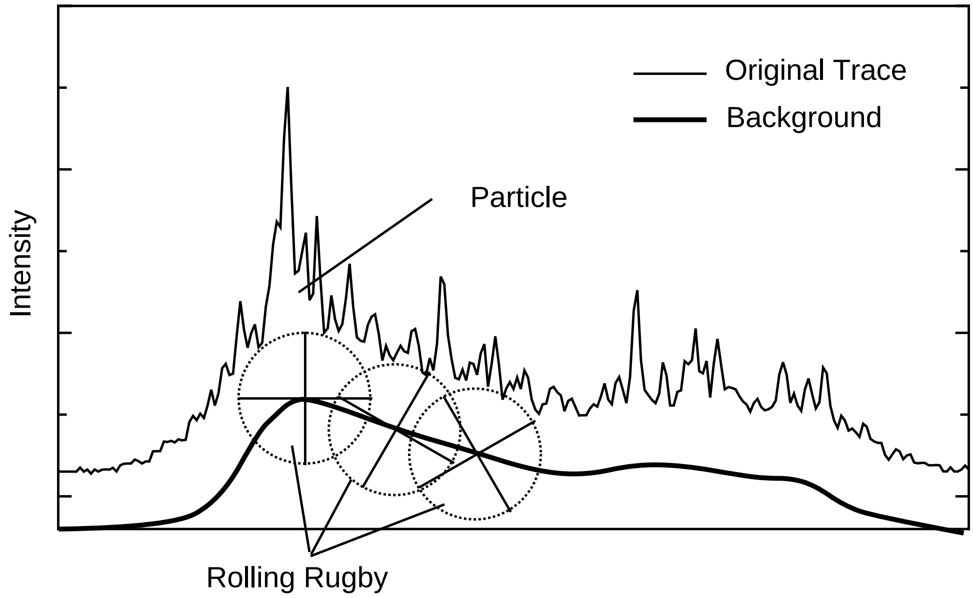

Figure 3 Intensity profile across the waterjet with rolling ball background

The remedy to this problem was to use an ellipsoid (= "rugby ball") instead of a sphere with its long axis parallel to the waterjet. Using a long axis of four times the average particle diameter and a short axis of the same size as the width of the hills respectively the particle diameter, the particles were preserved and the hills removed as demonstrated in **Figure 4**.

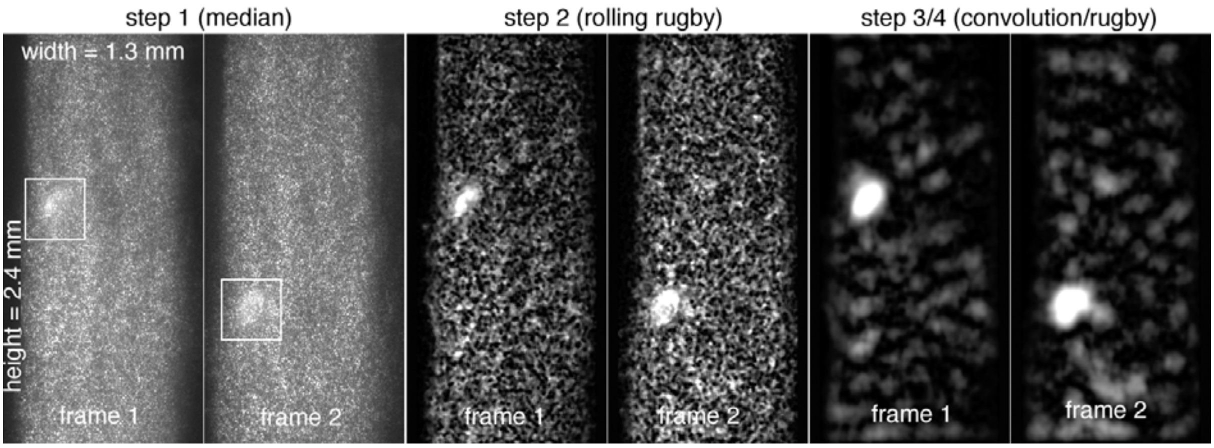

Figure 4 Typical intermediate and final results from our image processing program

A check by visual inspection showed that through these means about 90% of the particles could be detected while only few ghost particles where created. In order to avoid falsification of the statistics, all images with particle pairs where finally confirmed by visual inspection.

The displacement of the particle in pixels, obtained from the above described program, was finally converted to a real displacement by the use of a calibration image.

2.4 Measurement arrangement

For this measurement a test plant was designed and built (**Figure 5**). A standard abrasive water jet system was used with a pressure intensifier operating from 25MPa to 350MPa. With a 0.2mm diameter orifice and a 0.76mm diameter focusing tube the abrasive water jet was formed. The mesh size of the abrasive particles was 120.

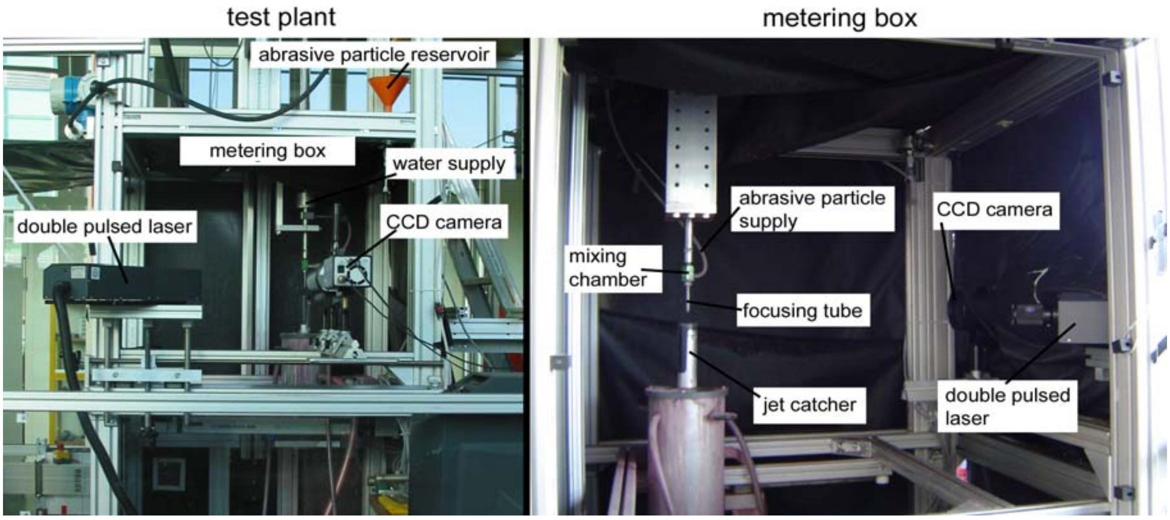

Figure 5 Test plant

The metering box was completely shielded against the environment to avoid interference. The pulsed laser and the CCD camera were focused on the water jet. Both the abrasive and the water mass flow rate were determined by volumetric measurement.
Investigated were two different water pressures, 250MPa and 345MPa, with five different abrasive mass flow rates at each pressure.

3 RESULTS

3.1 Definitions

The analysis was accomplished using dimensionless representation. For this, several reference values are defined. The particle velocity is referenced with the water jet velocity downstream from the orifice. Neglecting the compressibility of the water, the velocity is computed by Bernoulli's equation:

$$v_{ref} = \sqrt{\frac{2 \cdot p}{\rho}} \qquad (3)$$

We define a velocity ratio *VR*

$$VR := \frac{v}{v_{ref}} \qquad (4)$$

and a dimensionless mass flow *M* by forming the ratio between abrasive and water jet mass flow rates:

$$M := \frac{\dot{m}_{abr}}{\dot{m}_{jet}} \tag{5}$$

The velocity for a parameter set is analyzed by using the RMS-value of the measured velocities:

$$v_{eff} = \sqrt{\frac{1}{N} \cdot \sum_{i=1}^{N} v_i^{\,2}} \tag{6}$$

with N standing for the number of detected particles. This processing is used to include the quadratic influence of the velocity on the erosion process.

To analyze the process, the stationary momentum balance for the cutting head is applied in integral form assuming no body or surface forces:

$$\sum_{inlet} \dot{m} \cdot \vec{v} = \sum_{outlet} \dot{m} \cdot \vec{v} \tag{7}$$

By disregarding the air mass flow and the inlet velocity of the abrasive particles and assuming one-dimensional conditions, the momentum balance can be written as:

$$\dot{I}_{jet,inlet} = \dot{I}_{jet,outlet} + \dot{I}_{abr,outlet} \tag{8.a}$$

$$\dot{m}_{jet,inlet} \cdot \overline{v}_{jet,inlet} = \dot{m}_{jet,outlet} \cdot \overline{v}_{jet,outlet} + \dot{m}_{abr,outlet} \cdot \overline{v}_{abr,outlet} \tag{8.b}$$

The inlet velocity of the water jet is computed using equation (3).

The ratio of the momentum flux of the abrasive particles at the outlet and the momentum flux of the water jet at the inlet is used for quantifying the *process effectiveness* η:

$$\eta := \frac{\dot{I}_{abr,outlet}}{\dot{I}_{jet,inlet}} \tag{9}$$

For both the particle velocity and the ratio of momentum flux a theoretical maximum can be calculated assuming that the particle velocity is equal to the water jet velocity. This assumption combined with equation (8.b) leads to the *limit value for the particle velocity*:

$$\overline{v}_{abr,\max} = \frac{\dot{m}_{jet,inlet} \cdot \overline{v}_{jet,inlet}}{\dot{m}_{jet,outlet} + \dot{m}_{abr,outlet}} \tag{10}$$

The theoretical limit for the process effectiveness can now be computed using the maximal particle velocity given by equation (10):

$$\eta_{\max} = \frac{\dot{m}_{abr,outlet} \cdot \overline{v}_{abr,\max}}{\dot{m}_{jet,inlet} \cdot \overline{v}_{jet,inlet}} \tag{11}$$

3.2 Particle velocity distribution at the exit of focusing tube

The determined velocities of the detected particles were analyzed statistically and plotted as histogram. As shown in **Figure 6**, a typical Gaussian distribution results.

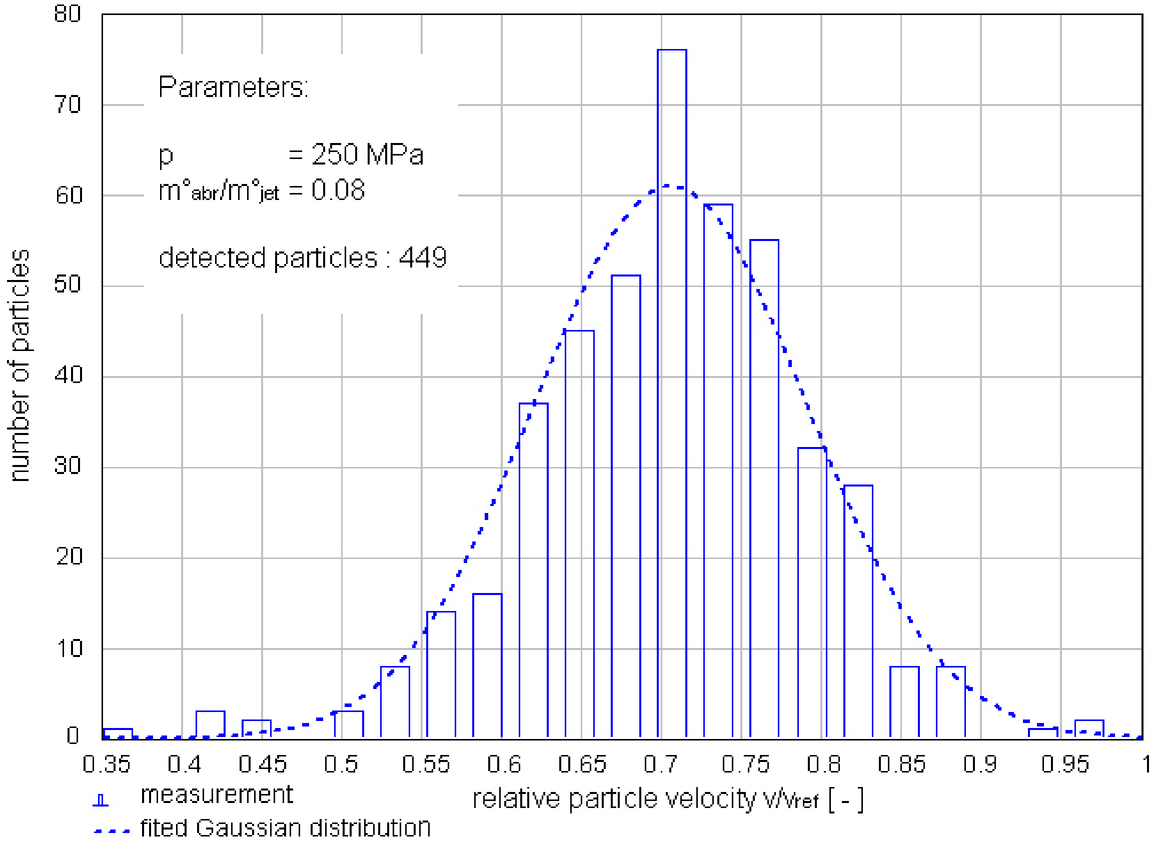

Figure 6 Particle velocity distribution

From the standard deviation and the number of detected particles the *uncertainty* of the mean particle velocity was computed. In our experiments it constitutes typically less than one percent and is not considered in the following plots.

3.3 Particle velocity dependence on abrasive mass flow and pressure

The interpretation of the measured data sets was done by correlating the RMS velocity ratio *VR* with the mass flow ratio *M* and setting the pressure as a parameter.

As shown in **Figure 7** the relative particle velocities decrease with increasing mass flow ratio. In the range which was investigated, a linear reduction of the mean velocity ratio with increasing mass flow ratio can be assumed. Because the pressure does not influence the relative particle velocity, it can be deduced that the absolute particle velocity rises with the square root of the pressure.

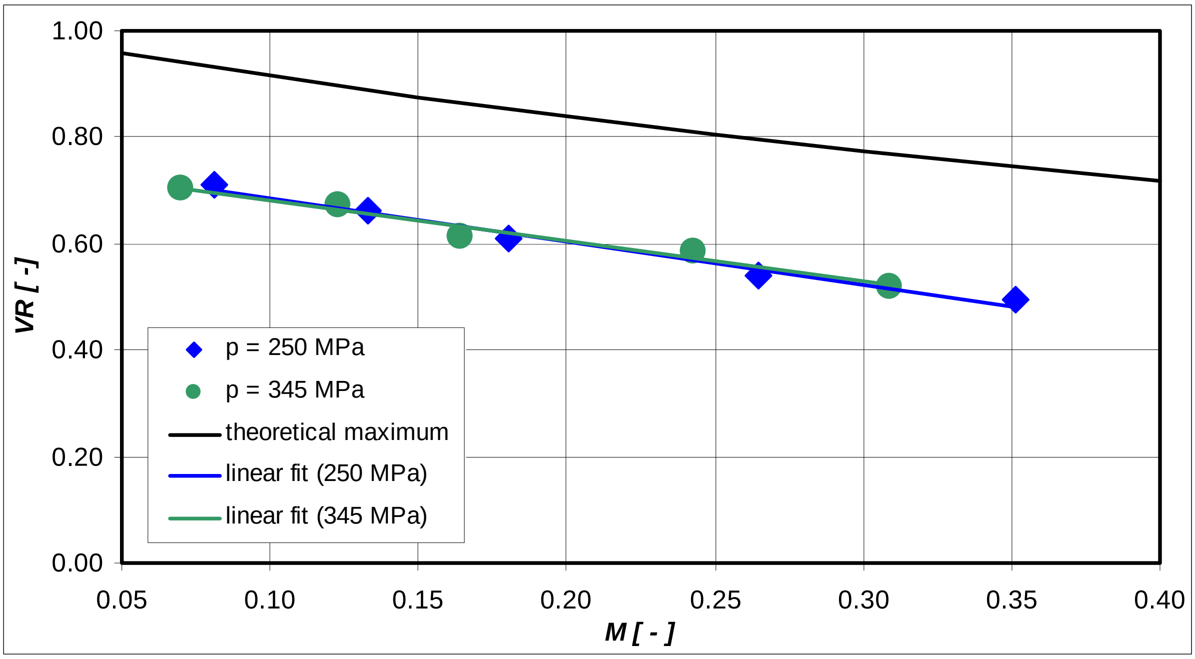

Figure 7 Relative particle velocity

3.4 Process effectiveness

The process effectiveness was determined using equation (9). In **Figure 8** η is plotted in function of the mass flow ratio. The pressure was again used as the parameter.

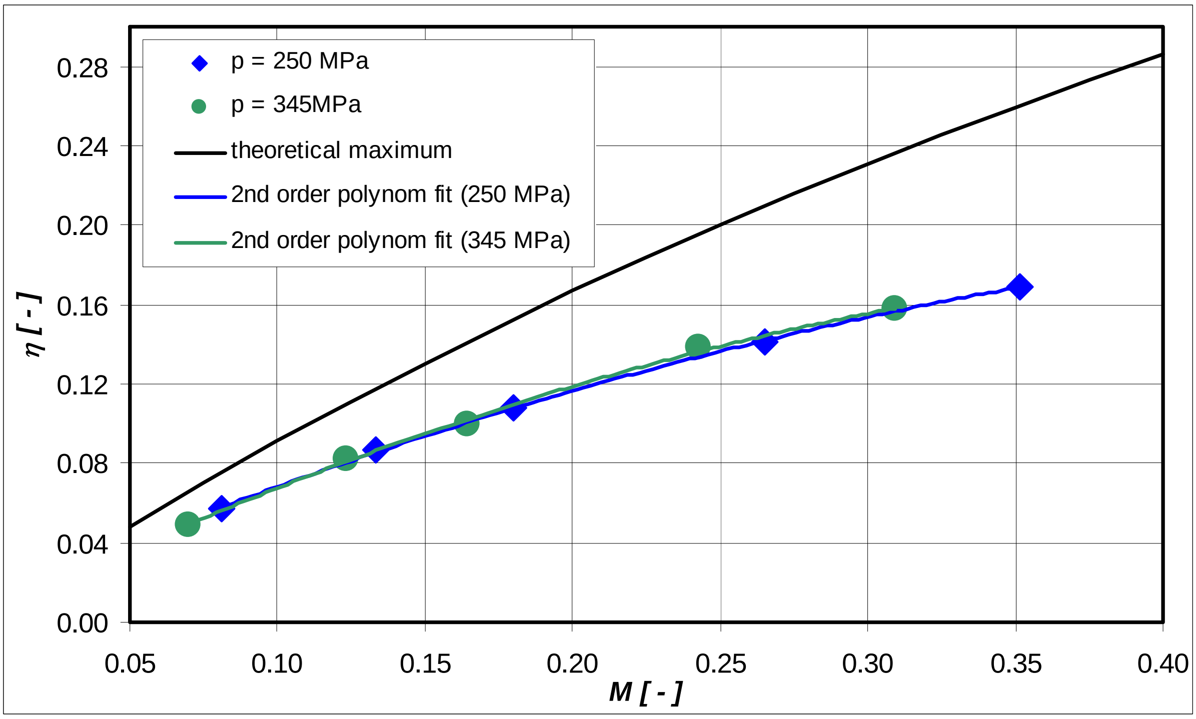

Figure 8 Process effectiveness (ratio of momentum fluxes)

While increasing the mass flow ratio, the process effectiveness rises. But as can be seen in Fig. 8 the *losses* increase as well when cutting with higher mass flow rates. This can be explained by the increasing internal friction in the focusing tube, which is caused by the augmented density due to the presence of particles. Again it can be seen that the pressure does not affect the process effectiveness.

4 CONCLUSIONS

The presented new technique is capable of measuring the velocity of abrasive particles in AWJ cutting in a wide range of cutting parameters under real conditions. Problems occur only for abrasive mass flow rates over 500g/min due to the formation of dense fog around the water jet.

As surmised before the onset of our experiments, the results confirm the following:

- The particle velocity increases with the water pressure
- The particle velocity decreases with the abrasive mass flow rate

Additionally, some new conclusions about the AWJ cutting process can be drawn:

- The losses due to internal friction are augmented with increasing mass flow rate
- In the investigated range there is no influence of the water pressure either on the relative momentum exchange between water jet and abrasive particles or on the relative particle velocity

5. REFERENCES

[1] M. Hashish
A Modeling study of metal cutting with abrasive water jets
Trans. ASME, Vol. 106, 1984, pp. 88-100

[2] J. G. A. Bitter
A study of Erosion phenomena - Part 1
Wear, Vol. 6, 1963, pp. 5-21

[3] M. Hashish
Measurement of abrasive-waterjet particle velocities
Flow industries, Inc., Corporate Technology Laboratory, Washington, 1985

[4] A. Dorle, L. J. Tyler, D. A. Summers
Measurement of particle velocities in high speed waterjet technology
University of Missouri, Rolla, 2003

[5] Y. Dong, L. J. Tyler, D. A. Summers, M. Johnson
Experimental study of particle velocity measurement in abrasive water jet cutting in the nozzle and jet stream using multiple sensing elements
University of Missouri, Rolla, 2004

[6] S. Sternberg
Biomedical Image Processing
University of Michigan, Ann Arbor, 1983

[7] http://rsb.info.nih.gov/ij/
Status 17. November 2004

6. ACKNOWLEGDEMENT

The authors would like to thank the Innovation Promotion Agency (CTI) of the Swiss Federal Office for Professional Education and Technology for supporting this project (No. 7495.1)

7. NOMENCLATURE

$\dot{m}_{jet}$	[g/min]	water jet mass flow
$\dot{m}_{abr}$	[g/min]	abrasive mass flow
p	[MPa]	water pressure
v_{jet}	[m/s]	water jet velocity
v_{abr}	[m/s]	abrasive particle velocity
$\dot{I}$	[N]	momentum flux
η	[-]	process effectiveness

8. GRAPHICS

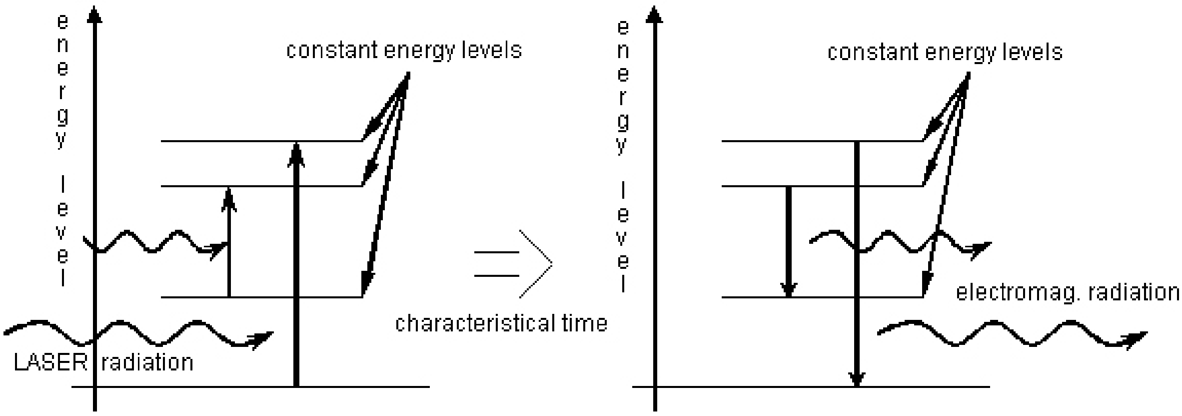

Figure 9 Fluorescence process